Searching For Resonances inside Top-like Events

Jared A. Evans,[1] Ben Kilminster,[2] Markus A. Luty,[3] and Daniel Whiteson[4]

[1] *NHETC, Rutgers University, Piscataway, New Jersey*
[2] *Fermi National Accelerator Laboratory, Batavia, Illinois*
[3] *University of California, Davis, Davis, California*
[4] *University of California, Irvine, Irvine, California*

In extended Higgs sectors, heavy Higgs bosons can decay via cascades to a light Higgs boson plus W and Z bosons. We study signals of such sectors at the Tevatron and LHC that result from resonant production of a heavy H^0 followed by the decay $H^0 \to H^\pm W^\mp$ with $H^+ \to W^+ h^0 \to W^+ b\bar{b}$ or $H^+ \to t\bar{b} \to W^+ b\bar{b}$. The final states have the same particle content as that of $t\bar{t}$ production, but with a resonant structure that can be used to distinguish signal events from background events. We propose analysis techniques and estimate the experimental sensitivity of the Tevatron and LHC experiments to these signals.

PACS numbers: 12.60.Fr, 14.65.Ha, 14.80.Fd, 14.80.Ec

I. INTRODUCTION

The experimental study of the electroweak symmetry breaking sector (or Higgs sector) is one of the main goals of the experimental high energy physics program. The minimal standard model with a single scalar Higgs boson is compatible with all existing data if the Higgs boson mass is in the range 115–140 GeV, and in fact intriguing hints of a Higgs boson with mass near 125 GeV have recently been found at the CERN Large Hadron Collider (LHC) [1, 2]. If a light Higgs-like state is definitively discovered, the next step in the experimental program will be to determine whether this state is in fact the Higgs boson of the minimal standard model, part of an extended Higgs sector (such as that of the minimal supersymmetric standard model, or MSSM [3]), a composite Higgs [4], or a completely different particle with Higgs-like couplings (such as a radion in warped extra dimensions [5] or dilaton [6]).

In this paper, we consider models with a light neutral Higgs boson that is part of an extended Higgs sector. Rather than assume a particular theoretical framework (such as the MSSM), we take a phenomenological approach, using a general 2-Higgs doublet model as a convenient simplified model [7] to parameterize the signals. This approach motivates a variety of signals with final states involving the heaviest standard model particles (W, Z, t, and b), which have the strongest couplings to the Higgs sector [8, 9]. The WW final state is enhanced by WW scattering in models where the Higgs sector is strongly coupled [10], and this signal has been the subject of much detailed investigation [11]. The phenomenology of resonant production of the final states Zh^0 [12] and W^+W^-Z [13] have also been investigated.

In this paper, we focus on the final state $W^+W^-b\bar{b}$, which can have a large production rate from the process $gg \to H^0$ followed by $H^0 \to H^\pm W^\mp$ with $H^+ \to W^+ h^0 \to W^+ b\bar{b}$ or $H^+ \to t\bar{b} \to W^+ b\bar{b}$. The main challenge with these signals is the large $t\bar{t}$ background, which shares the same final state. The Tevatron has performed in-depth studies of the properties of the top quark in the $t\bar{t}$ mode, including searches for charged Higgs bosons in top-quark decay [14], a measurement of the polarization of the top-quark decay products [15], and independent measurements of the top-quark mass in different top-quark decay modes [16]. The model considered in this paper can be viewed as a continuation of these investigations, understanding to what degree the $t\bar{t}$ sample at the Tevatron and the LHC can contain final states with a $b\bar{b}$ resonance.

This paper is organized as follows. In section II of the paper, we discuss a simplified model and Monte Carlo generation of the signal. In section III, we address selection criteria and the dominant backgrounds. Section IV and V discuss search strategies and expected sensitivity in $b\bar{b}$ and $Wb\bar{b}$ resonances respectively.

II. SIMPLIFIED MODEL

To carry out this study, we use a simplified model that contains only the minimal particle content necessary to describe the signal of interest. It contains two neutral Higgs bosons, heavy (H^0) and light (h^0), and two charged Higgs particles ($H^\pm$). The parameters of the model are simply the masses of the Higgses and the production cross section times branching ratios for the assumed decays. This allows for the simple interpretation of the parameters and the later mapping to the specific parameters of more complete theories.

The production mode studied here is gluon-gluon fusion $gg \to H^0$. We consider only the decay $H^0 \to H^\pm W^\mp$ and $h^0 \to b\bar{b}$. We consider two possible decays of the charge Higgs state, $H^+ \to W^+ h^0$ and $H^+ \to t\bar{b}$, performing two separate analyses for the limiting cases where one of these dominates. Although we are not committing to a specific model, it is worth noting that in 2-Higgs doublet models, these decays are controlled by the couplings

$$g_{H^+W^-h^0} = \frac{2m_Z \cos(\beta-\alpha)}{v\cos\theta_W}, \quad g_{H^+\bar{t}b} = \frac{m_t}{v\tan\beta}, \qquad (1)$$

which depend on different combinations of the angles α and β (defined for example in Ref. [17]). These searches therefore probe different regions of parameter space of this model. On the other hand, the production cross section depends on the coupling

$$g_{H^0 t\bar{t}} = \frac{m_t \sin\alpha}{v \sin\beta}. \quad (2)$$

For parameters where this is unsuppressed, the $H^+ \to t\bar{b}$ decay is also unsuppressed, so in a 2-Higgs doublet model the modes $H^+ \to W^+ h^0$ and $H^+ \to t\bar{b}$ are always both allowed. Nevertheless, we will study these modes independently in this preliminary study.

To avoid unnecessary model-dependent assumptions in our results, we give expected limits on the H^0 production cross section times the product of the appropriate branching ratios. To interpret the results, we need to know the expected rates in some reasonable models, so we give the cross section for H^0 production in Fig. 1, which is equivalent to the SM Higgs production cross section if $\sin\alpha/\sin\beta = 1$.

Both signal and background events are generated with MADGRAPH [18], while top-quark and W boson decay, showering and hadronization is performed by PYTHIA [19]. We use PGS [20] tuned for Tevatron or ATLAS to provide detector simulation.

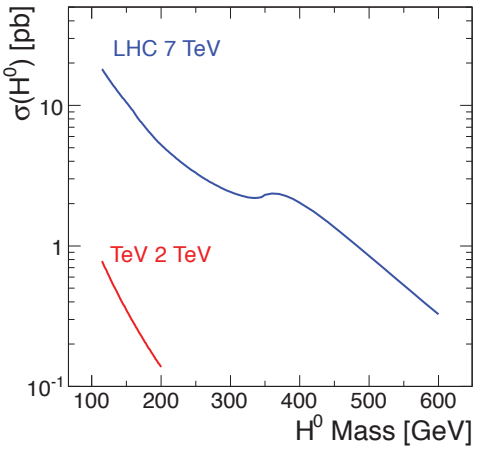

FIG. 1: Production cross section at NLO for H^0 as a function of mass in a 2-Higgs doublet model with $\sin\alpha/\sin\beta = 1$, equivalent to the SM Higgs production cross section, for Tevatron $p\bar{p}$ collisions at $\sqrt{s} = 1.96$ TeV [21], and for LHC pp collisions at $\sqrt{s} = 7$ TeV [22].

III. SELECTION AND BACKGROUNDS

The event selection is similar to the standard single lepton selection used for Tevatron and LHC measurements [23, 24] of the $t\bar{t} \to W^+\bar{b}W^-b$ final states, with one W boson decaying leptonically. We require:

- exactly one electron or muon, with $p_T > 20$ GeV and $|\eta| < 2.5$
- at least four jets, each with $p_T > 20$ GeV and $|\eta| < 2.5$
- at least 20 GeV of missing transverse momentum
- at least one b-tagged jet

The b-tagging algorithm parametrized in PGS is 36% (44%) efficient per b-quark jet for the Tevatron (LHC). The dominant standard model background is $t\bar{t}$ production. At the Tevatron (LHC) W+jets contributes 25% (10%) after this selection. In this study, we consider only the $t\bar{t}$ background.

IV. RESONANCES IN $b\bar{b}$

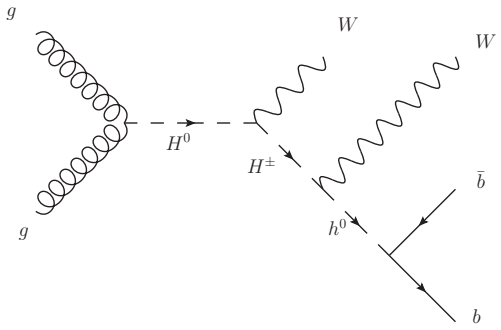

FIG. 2: Diagram for $WWb\bar{b}$ production via the cascade $gg \to H^0 \to H^\pm W^\mp \to WWh^0 \to WWb\bar{b}$

In this section, we discuss the search strategy for the cascade $gg \to H^0 \to H^\pm W^\mp \to W^+W^-h^0 \to W^+W^-b\bar{b}$. Events are reconstructed according to the $t\bar{t}$ hypothesis, in order to identify and remove this background. The neutrino transverse momentum is assumed to be given by the missing transverse momentum; the longitudinal component is assumed to the smallest value that gives $(p_\ell + p_\nu)^2 = m_W^2$. The pair of jets without b-tags that gives m_{jj} closest to m_W are labeled as the hadronic W boson decay products. In the case that the event contains exactly one b-tag, the leading untagged jet that is not associated to the hadronic W boson is treated as a second b-tagged jet. The two W bosons and b jets are paired to form hadronic and leptonic top quarks according to the assignment that minimizes $|M_t^{\rm lep} - M_t^{\rm had}|$ where M_t is the Wb invariant mass.

The $t\bar{t}$ background shows clear peaks in M_t for both leptonic and hadronic modes, see Fig. 3. The Higgs cascade decay lacks the top-quark resonance, leading to reconstructed top-quark masses further from the top-quark mass. To reduce the $t\bar{t}$ background, we veto events if $M_{Wb}^{\rm lep} \in [M-10, M+10]$ or $M_t^{\rm had} \in [M-10, M+10]$,

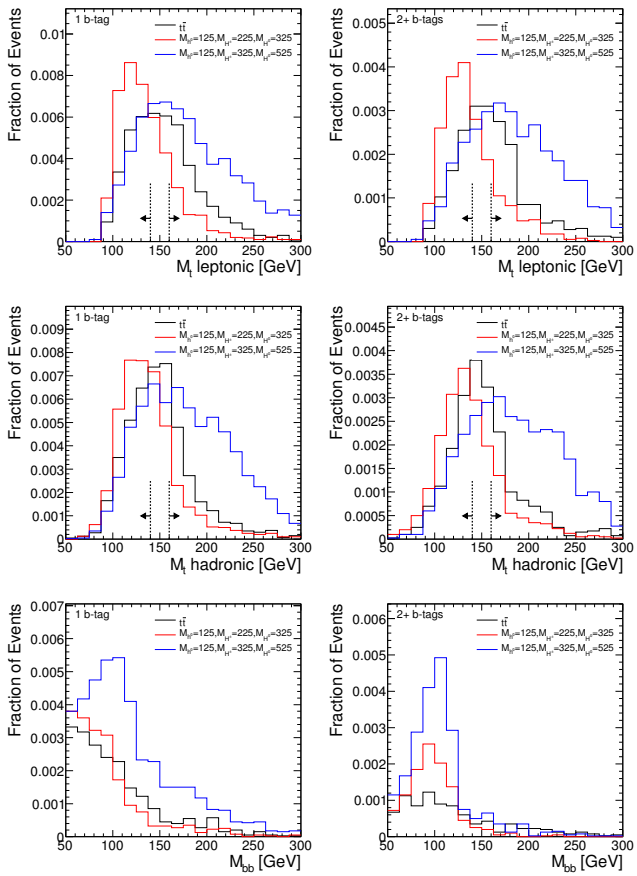

FIG. 3: Expected kinematic features from the $W^+W^-h^0 \to W^+W^-b\bar{b}$ signal shown with primary $t\bar{t}$ background at the Tevatron. Shown are the masses reconstructed as leptonic top (top), hadronic top (center) and the $b\bar{b}$ invariant mass (bottom). Events are categorized by the the number of b-tags seen: left is exactly one tag, right is at least two tags. The top-quark pair background in the $b\bar{b}$ mass distribution is suppressed by a top-quark veto, shown in the M_t distributions.

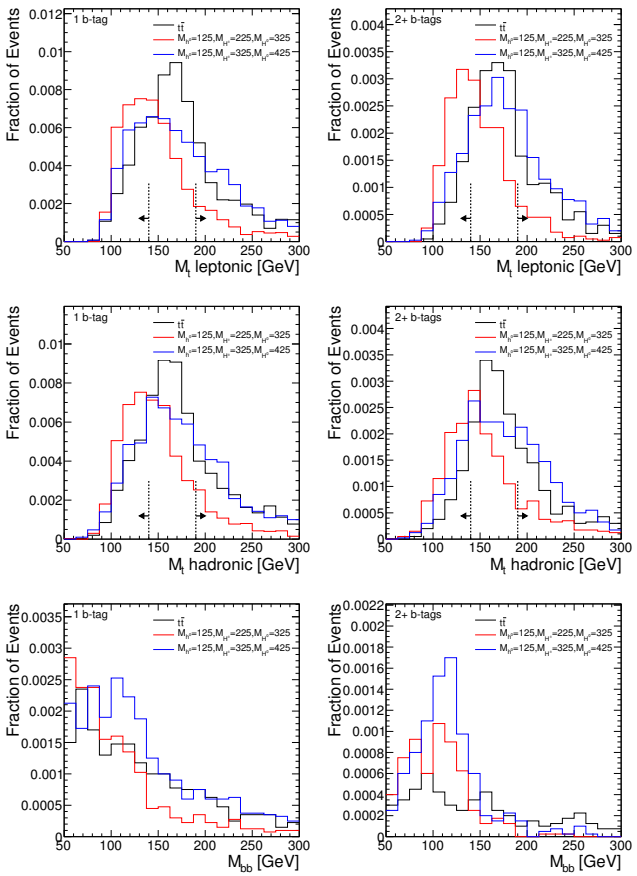

FIG. 4: Expected kinematic features from the $W^+W^-h^0 \to W^+W^-b\bar{b}$ signal shown with primary $t\bar{t}$ background at the LHC. Shown are the masses reconstructed as leptonic top (top), hadronic top (center) and the $b\bar{b}$ invariant mass (bottom). Events are categorized by the the number of b-tags seen: left is exactly one tag, right is at least two tags. The top-quark pair background in the $b\bar{b}$ mass distribution is suppressed by a top-quark veto, shown in the M_t distributions.

where M is the median reconstructed top-quark mass in simulated $t\bar{t}$ events, and the window size is optimized to maximize expected sensitivity.

For the signal, the h^0 mass is formed by M_{bb} and shows a clear peak in simulated Higgs cascade events, see Fig. 3.

A similar strategy is followed for LHC analysis, see Fig. 4, with a wider top-quark veto $[M-25, M+25]$ to suppress the larger top-quark rate at the LHC.

One could further improve the background rejection by searching for the $H^\pm$ resonance in m_{Wbb}, or the H^0 resonance in m_{WWbb}, see Fig. 5. The sensitivity gain may be modest, as the m_{bb} spectrum provides powerful discrimination between the signal and background shapes while further selection requirements would reduce the signal acceptance. A two-dimensional analysis of m_{bb} versus m_{WWbb} is likely to be most effective. The simple one-dimensional analysis performed here is sufficient to demonstrate sensitivity.

The expected background levels are calculated using the NLO cross section [25] for the $t\bar{t}$, acceptance calculated with simulated events, and a luminosity of 8 fb^{-1} (5 fb^{-1}) for the Tevatron (LHC). A 10% uncertainty is assumed. The signal acceptance is calculated using simulated events, see Figs. 6a & 7a.

To extract the most likely value of the signal cross section, we analyze the shape of the m_{bb} distribution. Specifically, a binned maximum likelihood fit is used in the m_{bb} variable, floating each background rate within uncertainties, allowing variation due to systematic uncertainties described above. The signal and background rates are fit simultaneously. The top-quark mass veto described above improves the sensitivity by approximately 20%, by significantly reducing the background efficiency relative to the signal efficiency. The CLs method [26] is used to set 95% cross section upper limits. The median expected upper limit is extracted in the background-only

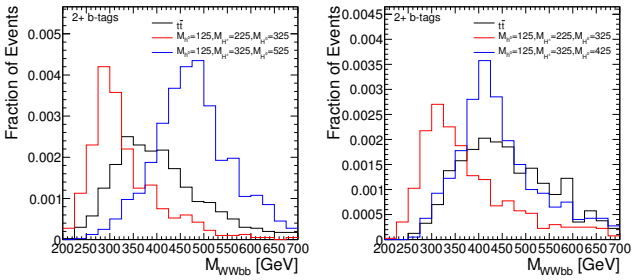

FIG. 5: Reconstruction of the total invariant mass of the $H^0 \to H^\pm W^\mp \to W^+W^-h^0 \to W^+W^-b\bar{b}$ cascade, as m_{WWbb}. Left is for the Tevatron; right, LHC.

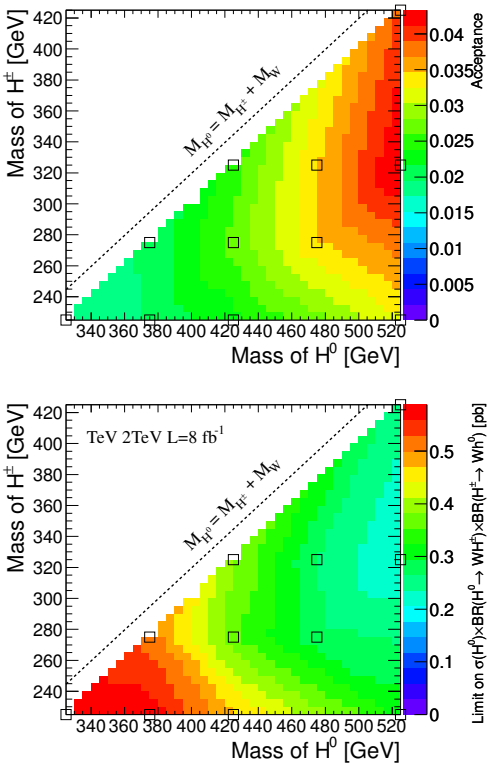

FIG. 6: Signal acceptance and expected limits at the Tevatron: top (a) is $W^+W^-h^0 \to W^+W^-b\bar{b}$ signal acceptance after top-quark veto, including the branching ratio $WW \to \ell\nu qq'$; bottom (b) is the median expected 95% CL upper limits in the background-only hypothesis. Both panes use $h^0 = 125$ GeV, and varying H^0 and $H^\pm$ masses.

hypothesis, see Figs. 6b & 7b.

V. RESONANCES IN Wbb

Production of $W^+W^-b\bar{b}$ may also occur through the cascade process (Fig. 8),

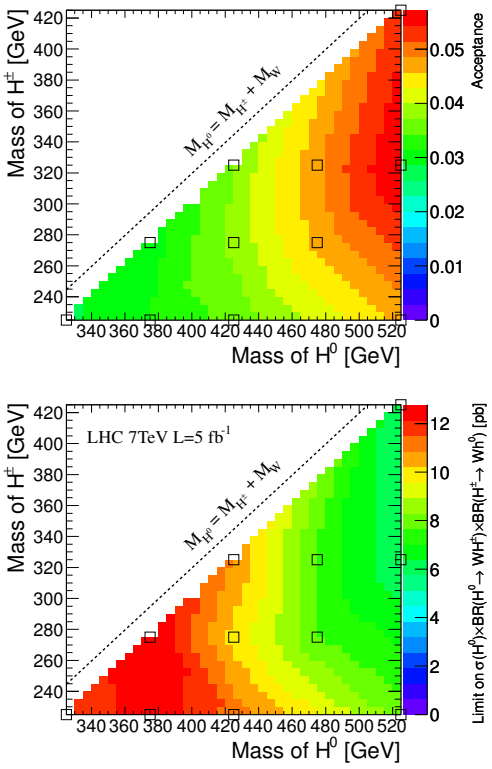

FIG. 7: For the LHC: top (a) is $W^+W^-h^0 \to W^+W^-b\bar{b}$ signal acceptance after top-quark veto, including the branching ratio $WW \to \ell\nu qq'$. Bottom (b) is median expected 95% CL upper limits in the background-only hypothesis. Both panes use $h^0 = 125$ GeV, and varying H^0 and $H^\pm$ masses.

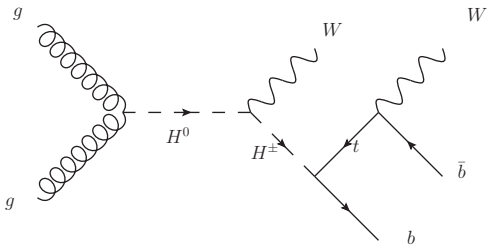

FIG. 8: Diagram for $W^+W^-b\bar{b}$ production via the cascade $gg \to H^0 \to H^\pm W^\mp \to Wtb \to W^+W^-b\bar{b}$.

$$gg \to H^0 \to H^\pm W^\mp \to Wtb \to W^+W^-b\bar{b}$$

which gives resonant production of $H^\pm \to W^\pm b\bar{b}$, and kinematics distinct from $t\bar{t} \to W^+W^-b\bar{b}$.

As in the $b\bar{b}$ resonance case, events are reconstructed according to the $t\bar{t}$ hypothesis, in order to identify and remove this background. The $t\bar{t}$ background shows clear peaks in M_t for both leptonic and hadronic modes, see Fig. 3. The Higgs cascade decay has exactly one top-

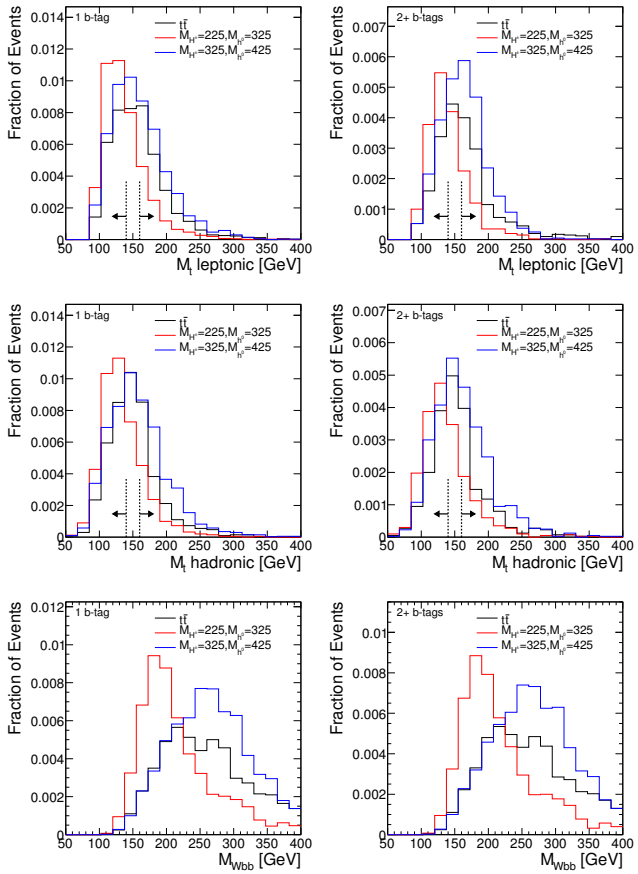

FIG. 9: Expected kinematic features of $H^{\pm} \to W^{\pm} b\bar{b}$ resonance signal and background events at the Tevatron. Shown are leptonic top mass (top), hadronic top mass (center) and $Wb\bar{b}$ invariant mass (bottom). Events are categorized by the the number of b-tags seen: left is exactly one tag, right is at least two tags. The top-quark pair background in the $Wb\bar{b}$ mass distribution is suppressed by a top-quark veto, shown in the M_t distributions.

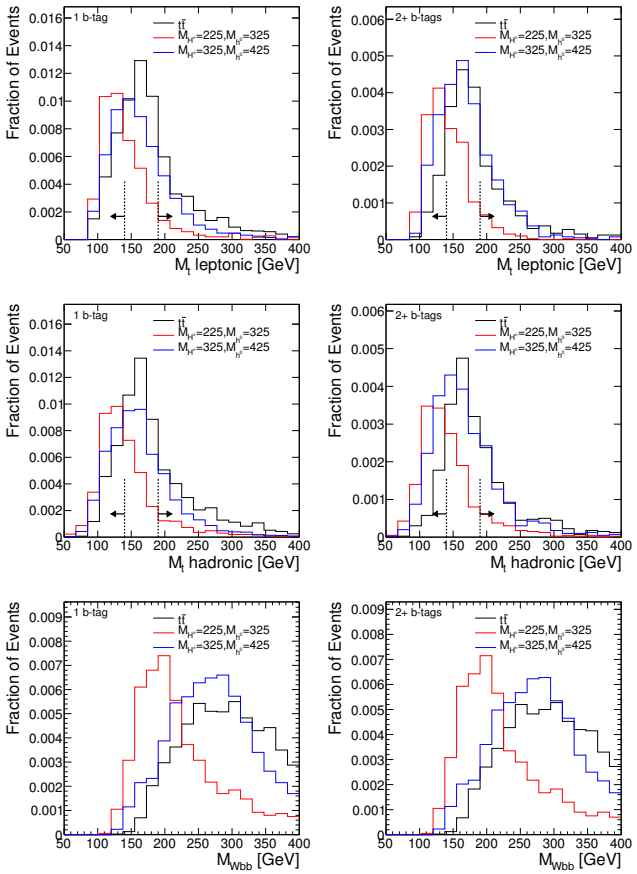

FIG. 10: Expected kinematic features of $H^{\pm} \to W^{\pm} b\bar{b}$ resonance signal and background events at the LHC. Shown are leptonic top mass (top), hadronic top mass (center) and $Wb\bar{b}$ invariant mass (bottom). Events are categorized by the number of b-tags seen: left is exactly one tag, right is at least two tags. The top-quark pair background in the $Wb\bar{b}$ mass distribution is suppressed by a top-quark veto, shown in the M_t distributions.

quark decay, leading to reconstructed top-quark masses that are broader than in the background SM top-quark pair production, but more difficult to discriminate from $t\bar{t}$ than the $b\bar{b}$ case which has no top quarks. To reduce the $t\bar{t}$ background, we veto events if $M_t^{\rm lep} \in [M-10, M+10]$ **and** $M_t^{\rm had} \in [M-10, M+10]$, where M is the median reconstructed M in simulated $t\bar{t}$ events, and the window size is optimized to maximize expected sensitivity.

The resonance mass is formed by m_{Wbb}, choosing the W boson that gives the largest value of m_{Wbb}. It shows a clear peak in simulated Higgs cascade events, see Fig. 9. As for the $b\bar{b}$ resonance, one could likely further improve the background rejection by using the H^0 resonance in m_{WWbb} as a second analysis dimension, see Fig. 11.

Signal and background yields are calculated as in the $b\bar{b}$ case described above. The signal acceptance is calculated using simulated events, see Figs. 12a & 13a. The median expected upper limit is extracted in the background-only hypothesis, see Figs. 12b & 13b.

VI. CONCLUSIONS

Extended Higgs sectors can produce Higgs cascade decays leading to a $W^+W^-\bar{b}b$ final state that appears in top-quark pair production. We have shown that the resonance structure of the Higgs cascade decays can be used to distinguish these experimentally. The investigation here uses only the $\bar{b}b$ invariant mass, while the reconstructed masses of the H^0 and $H^{\pm}$ particles in the cascade may also be useful.

The M_t distributions, which are the primary reconstructed quantities used in top-quark mass measurements, appear different for the signals discussed than for the $t\bar{t}$ background. Therefore, should the above signals exist, contamination in the $W^+W^-b\bar{b}$ final states

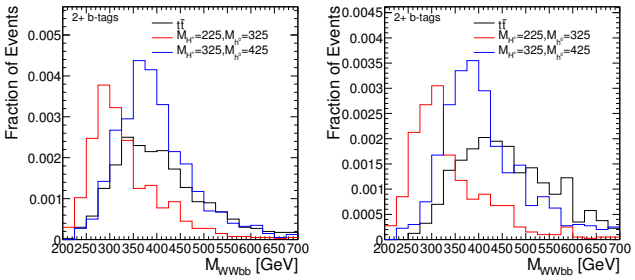

FIG. 11: Reconstruction of the total invariant mass of the $H^0 \to H^\pm W^\mp \to Wtb \to W^+W^-b\bar{b}$ cascade, as m_{WWbb}. Left is Tevatron, right is LHC.

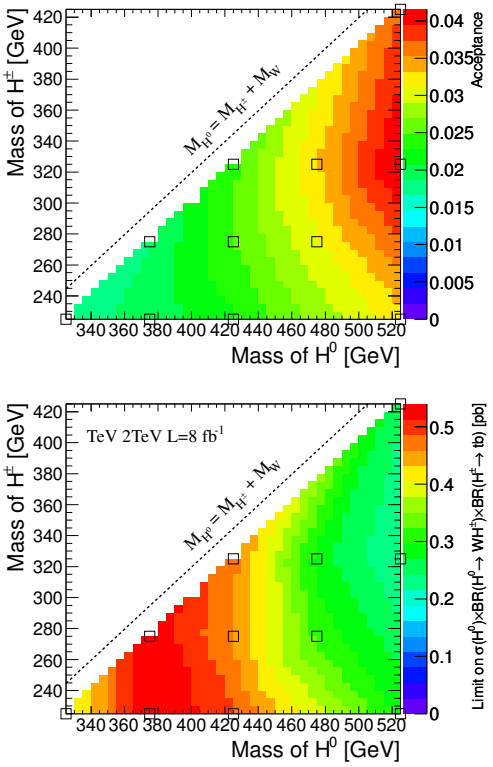

FIG. 12: For the Tevatron: top (a) is $H^\pm \to W^\pm b\bar{b}$ signal acceptance after top-quark veto, including the branching ratio $W^+W^- \to \ell\nu qq'$. Bottom (b) is median expected 95% CL upper limits in the background-only hypothesis.

would lead to measurements of the top-quark mass yielding artificially high or low values, depending on the exact mass hierarchy of the H^0 and $H^\pm$. This could generate perceived tension in the standard model precision electroweak fits which use the top-quark mass in order to determine the most likely Higgs boson mass. Study of the $t\bar{t}$ final states proposed here could disentangle these effects.

The simple approach presented in this work is sufficient

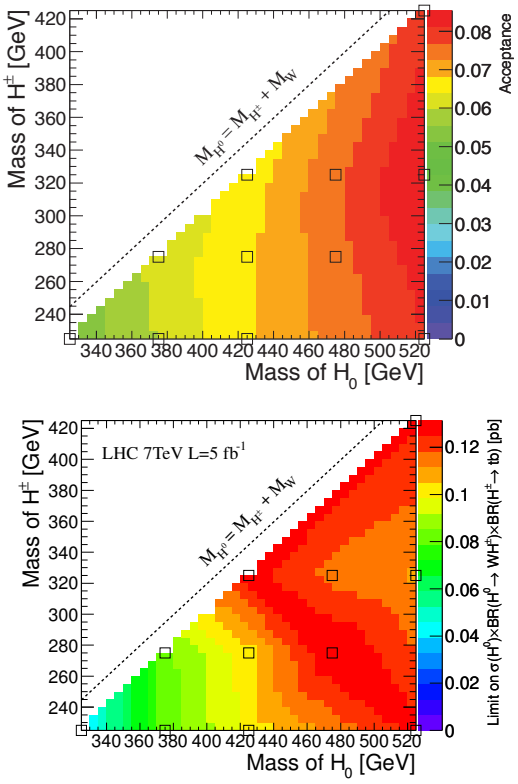

FIG. 13: For the LHC: top (a) is $H^\pm \to W^\pm b\bar{b}$ signal acceptance after top-quark veto, including the branching ratio $W^+W^- \to \ell\nu qq'$. Bottom (b) is median expected 95% CL upper limits in the background-only hypothesis.

to demonstrate that both the Tevatron and the LHC have sensitivity to these processes, and we leave a more sophisticated analysis for the actual experimental searches.

VII. ACKNOWLEDGEMENTS

We thank Will Shepherd, David Shih and Scott Thomas for useful conversations. The authors are supported by grants from the Department of Energy Office of Science and by the Alfred P. Sloan Foundation.

[1] The ATLAS Collaboration, ATLAS-CONF-2011-163, https://cdsweb.cern.ch/record/1406358

[2] The CMS Collaboration, CMS-PAS-HIG-11-032, https://cdsweb.cern.ch/record/1406347

[3] H. P. Nilles, Phys. Rept. **110** 1-162 (1984); H. E. Haber and G. L. Kane, Phys. Rept. **117** 75-263 (1985).

[4] D. B. Kaplan and H. Georgi, Phys. Lett. **B136**, 183 (1984).

[5] C. Csaki, M. Graesser, L. Randall and J. Terning, Phys. Rev. D **62**, 045015 (2000) [arXiv:hep-ph/9911406]; G. F. Giudice, R. Rattazzi and J. D. Wells, Nucl. Phys. B **595**, 250 (2001) [arXiv:hep-ph/0002178].

[6] W. D. Goldberger, B. Grinstein and W. Skiba, Phys. Rev. Lett. **100**, 111802 (2008) [arXiv:0708.1463].

[7] D. Alves *et al.*, [arXiv:1105.2838];

[8] J. A. Evans and M. A. Luty, Phys. Rev. Lett. **103**, 101801 (2009).

[9] S. Chang, J. A. Evans, and M. A. Luty, simplified model "Multiple Weak Bosons from Strong Spin-0 Resonances," `http://lhcnewphysics.org/leptons`.

[10] B. W. Lee, C. Quigg and H. B. Thacker, Phys. Rev. **D16**, 1519 (1977); M. S. Chanowitz and M. K. Gaillard, Nucl. Phys. **B261**, 379 (1985).

[11] J. Bagger *et al.*, Phys. Rev. **D52**, 3878 (1995); J. M. Butterworth, B. E. Cox and J. R. Forshaw, Phys. Rev. **D65**, 096014 (2002);

[12] S. Abdullin, H. Baer, C. Kao, N. Stepanov, and X. Tata, Phys. Rev. D **54**, 6728 (1996).

[13] S. Chang, J. Evans and M. Luty, Phys. Rev. **D84**, 095030 (2011).

[14] CDF Collaboration, Phys. Rev. Lett. **103**, 101803 (2009); D0 Collaboration, Phys. Lett. **B682**, 278-286 (2009).

[15] CDF Collaboration, Phys. Rev. **D83**, 112003 (2011); D0 Collaboration, [arXiv:1107.4995].

[16] Tevatron EWWG, FERMILAB-TM-2504-E, [arXiv:1107.5225].

[17] J. Gunion *et al.*, "The Higgs Hunter's Guide", Addison-Wesley, Redwood City (1990).

[18] J. Alwall et al., JHEP **0709** 028 (2007).

[19] T. Sjöstrand *et al.*, Comput. Phys. Commun. **135** (2001) 238 T. Sjöstrand, Comput. Phys. Commun. **82**, 74 (1994).

[20] J. Conway, `http://www.physics.ucdavis.edu/conway/research/software/pgs/pgs.html`

[21] The Higgs Working Group, arXiv:hep-ph/0406152 (2003)

[22] LHC Higgs Cross Section Working Group, arXiv:1101.0593v3 (2011).

[23] CDF Collaboration, Phys. Rev. Lett. **97**, 082004 (2006); D0 Collaboration, Phys. Rev. **D76**, 092007 (2007).

[24] ATLAS Collaboration, Eur. Phys. J. C **71** (2011) 1577; CMS Collaboration, Eur. Phys. J. C **71** (2011) 1721.

[25] M. Aliev et al., HATHOR HAdronic Top and Heavy quarks crOss section calculatoR, arXiv:1007.1327 [hep-ph].

[26] A. Read, J. Phys. G: Nucl. Part. Phys. **28** (2002) 2693; T. Junk, Nucl. Instr. Meth. A **434** (1999) 435.